Research in Astron. Astrophys. **2013** Vol. **13** No. **5**, 579–592
http://www.raa-journal.org *http://www.iop.org/journals/raa*

***R**esearch in*
***A**stronomy and*
***A**strophysics*

Grids of rotating stellar models with masses between 1.0 and 3.0 $M_\odot$ *

Wu-Ming Yang[1,2], Shao-Lan Bi[1] and Xiang-Cun Meng[2]

[1] Department of Astronomy, Beijing Normal University, Beijing 100875, China; *yangwuming@ynao.ac.cn; yangwuming@bnu.edu.cn*
[2] School of Physics and Chemistry, Henan Polytechnic University, Jiaozuo 454000, China

Received 2012 November 5; accepted 2012 November 30

Abstract We calculated a grid of evolutionary tracks of rotating models with masses between 1.0 and 3.0 $M_\odot$ and resolution $\delta M \leq 0.02\,M_\odot$, which can be used to study the effects of rotation on stellar evolution and on the characteristics of star clusters. The value of $\sim 2.05\,M_\odot$ is a critical mass for the effects of rotation on stellar structure and evolution. For stars with $M > 2.05\,M_\odot$, rotation leads to an increase in the convective core and prolongs their lifetime on the main sequence (MS); rotating models evolve more slowly than non-rotating ones; the effects of rotation on the evolution of these stars are similar to those of convective core overshooting. However for stars with $1.1 < M/M_\odot < 2.05$, rotation results in a decrease in the convective core and shortens the duration of the MS stage; rotating models evolve faster than non-rotating ones. When the mass has values in the range $\sim 1.7 - 2.0\,M_\odot$, the mixing caused by rotationally induced instabilities is not efficient; the hydrostatic effects dominate processes associated with the evolution of these stars. For models with masses between about 1.6 and $2.0\,M_\odot$, rotating models always exhibit lower effective temperatures than non-rotating ones at the same age during the MS stage. For a given age, the lower the mass, the smaller the change in the effective temperature. Thus rotations could lead to a color spread near the MS turnoff in the color-magnitude diagram for intermediate-age star clusters.

Key words: stars: evolution — stars: rotation — stars: interiors

1 INTRODUCTION

Recently, it has been discovered that some intermediate-age star clusters have double or extended main-sequence turnoffs (MSTOs) in their color-magnitude diagrams (CMDs) (Mackey & Broby Nielsen 2007; Mackey et al. 2008; Milone 2009; Goudfrooij et al. 2009, 2011). Platais et al. (2012) also found that the upper main sequence of the open cluster Trumpler 20 with an age of about 1.3 Gyr appears to show an enlarged color spread which is not normally seen in the CMD for open clusters in this age group. The double or extended MSTOs are interpreted as star clusters that have two or multiple stellar populations with similar metal abundance but with differences in age of ∼200–300 Myr (Mackey et al. 2008), which is contrary to the traditional knowledge that a star cluster is comprised of stars belonging to a single, simple stellar population with a uniform age and chemical composition.

∗ Supported by the National Natural Science Foundation of China.

However, Platais et al. (2012) also pointed out that the enlarged color spread of Trumpler 20 may be due to differential reddening. In order to understand the extended MSTO, many scenarios have been proposed by investigators (Mackey & Broby Nielsen 2007; Bekki & Mackey 2009; Goudfrooij et al. 2009; Bastian & de Mink 2009; Rubele et al. 2010; 2011; Yang et al. 2011b; Girardi et al. 2011). In these scenarios, Yang et al. (2011b) found that the interactions in binary systems can reproduce an extended MSTO of star clusters. However, the fraction of interacting binary systems is too low to completely explain the observed features in star clusters. Another interpretation proposed by Rubele et al. (2010; 2011) and Girardi et al. (2011) is continuous star formation, lasting $\sim$300 Myr or longer. However, Platais et al. (2012) noted that "this long period of star formation seems to be at odds with the fact that none of the younger clusters are known to have such a trait" and that some star clusters with extended MSTO might not experience self-enrichment. Yang et al. (2011b) also noted that the length of time necessary to explain the double MSTO and dual red clump of a star cluster is not the same.

Rotation is a property that virtually all stars possess. Observations show that main-sequence (MS) stars with $1.3 < M/M_{\odot} < 3.0$ have a typical value of 160 km s^{-1} for $v \sin i$ (Royer et al. 2007) which corresponds to a period of $\sim$0.5–0.8 d. In the classical theory of stellar evolution, the effects of rotation are always neglected. However, rotation is one of the key factors that can change the evolution and resulting outputs of stellar models (Maeder & Meynet 2000). Bastian & de Mink (2009) calculated the evolutions of rotating models with an initial mass of 1.5 $M_{\odot}$ but with different rotation rates using the stellar evolution code described by Yoon et al. (2006) in which the effects of rotation on the structure and mixing induced by rotation are taken into account. They found that rotating models are cooler and fainter than non-rotating ones for rotation rates that are not extreme. They incorporated these effects of rotation on stellar evolution into the synthesis of CMDs for star clusters. They found that stellar rotations can mimic the effect of multiple populations in star clusters, whereas in actuality only a single population exists. However, using the Geneva stellar evolution code, Eggenberger et al. (2010) and Girardi et al. (2011) calculated the evolutions of rotating models with an initial velocity on the zero-age main sequence (ZAMS) of 150 km s^{-1} and found that rotating models can be slightly hotter and brighter than non-rotating ones. The isochrone of rotating stars has a slightly hotter and brighter turnoff with respect to that of non-rotating stars (Girardi et al. 2011), which is contrary to the calculation result of Bastian & de Mink (2009). The origin of the extended MSTO in intermediate-age star clusters is still an open question. In order to understand the effects of stellar rotation on the evolution of stars and on the CMD of star clusters, the evolution of rotating stars needs to be studied in more detail.

In this paper, we mainly focus on the effects of rotation on the evolution of stars, especially on the evolution of intermediate-mass MS stars which correspond to MSTO stars of intermediate-age star clusters. The paper is organized as follows: we give a physical description of the effects of rotation in Section 2, present the calculation results in Section 3 and discuss and summarize them in Section 4.

2 PHYSICAL DESCRIPTION OF ROTATION

2.1 Effects of Rotation on Stellar Structure and Evolution

The equations of stellar structure of a rotating star were proposed by Kippenhahn & Thomas (1970) and modified by Endal & Sofia (1976) and Meynet & Maeder (1997) to calculate shellular rotation. Rotation mainly affects stellar structure and evolution in four ways:

(1) The first is the effect of centrifugal force on the effective gravity. This effect can be considered directly in the equation of hydrostatic equilibrium.
(2) The second is that, for a rotating star, the equipotential or isobar surfaces are no longer spheres, because the centrifugal force is always perpendicular to the axis of rotation and is not, in general,

parallel to the force of gravity. Thus the assumption of spherical symmetry for non-rotating stars is no longer valid for rotating cases. A rotating star may be a spheroid. This leads to the fact that almost all structure equations are affected and the independent variables in equations describing stellar structure need to be redefined.

(3) The third is that the radiative flux is not constant on an isobaric surface because the radiative flux varies with the local effective gravity, i.e. the Von Zeipel effect (Von Zeipel 1924), which affects the radiative equilibrium equation and the instability of convection by changing the radiative temperature gradient.

(4) The final results from the transport of angular momentum and the mixing of elements caused by rotationally induced instabilities. The mixing happening in the stellar interiors can affect the density distribution by changing the mean molecular weight. Thus it can affect the radius of stars, the instability of convection, and so on.

The first three effects are directly incorporated into the equations of stellar structure (Endal & Sofia 1976). In a nonrotating model the independent variable, M_r, is the mass contained within a spherical surface. However, in a rotating one the independent variable, M_p, is the mass contained within an isobar surface. The algorithmic methods describing an isobaric surface and the physical quantities associated with it can be found in Endal & Sofia (1976), Meynet & Maeder (1997), and Yang & Bi (2006).

2.2 Angular Momentum Loss, Angular Momentum Transport and the Mixing of Elements

In this context, we assume that angular momentum loss is caused by magnetic stellar winds and the loss only happens when the stellar envelope is convective. The parameterized Kawaler's relations (Kawaler 1988; Chaboyer et al. 1995)

$$\frac{dJ}{dt} = f_k K_w \left(\frac{R}{R_\odot}\right)^{2-\beta} \left(\frac{M}{M_\odot}\right)^{-\beta/3} \left(\frac{\dot{M}}{10^{-14}}\right)^{1-2\beta/3} \Omega^{1+4\beta/3} \quad (\Omega < \Omega_{\rm crit}), \tag{1}$$

$$\frac{dJ}{dt} = f_k K_w \left(\frac{R}{R_\odot}\right)^{2-\beta} \left(\frac{M}{M_\odot}\right)^{-\beta/3} \left(\frac{\dot{M}}{10^{-14}}\right)^{1-2\beta/3} \Omega\Omega_{\rm crit}^{4\beta/3} \quad (\Omega \geq \Omega_{\rm crit}) \tag{2}$$

are used to calculate the rate of angular momentum loss, where f_k, β, and $\Omega_{\rm crit}$ are adjustable parameters, $K_w = 2.035 \times 10^{33} \times (1.442 \times 10^9)^\beta$ is in cgs units, and the mass-loss rate $\dot{M}$ is set to $2.0 \times 10^{-14}\, M_\odot\ {\rm yr}^{-1}$. The value of f_k calibrated to the Sun is 2.5, however, this may overestimate the rate of angular momentum loss for stars with mass larger than the Sun because these stars have a shallower convective envelope than the Sun. Thus we adopted a value of 1.0 for stars with mass larger than the Sun.

In addition, we assumed that the rotation is uniform on the ZAMS and in all convective regions of a star. The angular momentum loss, expansion and/or contraction of stars lead to the occurrence of differential rotation in radiative regions. The rotational instabilities induced by rotation can not only transport angular momentum but also mix chemical elements. Because the horizontal turbulence is stronger than the vertical turbulence, the angular velocity and chemical compositions are constant on an isobar (Zahn 1992). Thus we only consider the vertical transports of angular momentum and chemical elements which obey two coupled nonlinear diffusion equations

$$\rho r^2 \frac{I}{M} \frac{\partial \Omega}{\partial t} = f_\Omega \frac{\partial}{\partial r} \left(\rho r^2 \frac{I}{M} D \frac{\partial \Omega}{\partial r}\right) - \frac{\partial}{\partial r} \left(\rho r^2 \frac{I}{M} \Omega \dot{r}\right) \tag{3}$$

for the transport of angular momentum and

$$\frac{\partial X_i}{\partial t} = \left(\frac{\partial X_i}{\partial t}\right)_{\rm nuc} - \frac{1}{\rho r^2} \frac{\partial}{\partial r} \left(\rho r^2 X_i V_i\right) + f_\Omega \frac{1}{\rho r^2} \frac{\partial}{\partial r} \left(\rho r^2 f_c D \frac{\partial X_i}{\partial r}\right) \tag{4}$$

for the change in the the mass fraction X_i of species i, where the fraction I/M is the moment of inertia per unit mass, and D is the diffusion coefficient due to the rotational instabilities including meridional circulation, the Goldreich-Schubert-Fricke instability (Goldreich & Schubert 1967; Fricke 1968), and the secular shear instability. The criterion and the estimate of the coefficient D of these instabilities are summarized by Endal & Sofia (1978) and Pinsonneault et al. (1989). The second term on the right side of Equation (3) describes the change of angular velocity induced by contraction and/or expansion of stars. The first and second terms on the right side of Equation (4) are due to the nuclear reaction and gravity settling diffusion, respectively. The velocity, V_i, of the gravity settling diffusion is given by Thoul et al. (1994). The adjustable parameter f_Ω is introduced to represent some inherent uncertainties in the diffusion equation, and the f_c, which is less than one, is used to account for the fact that the transports of angular momentum and a chemical species occur on different timescales. The parameters f_Ω and f_c may depend on stellar mass. However, for simplicity, they are assumed to be constant. The values of the adjustable parameters in Equations (1)–(4) are summarized in Table 1. The effects of magnetic fields in the stellar interiors are not considered in our models. The magnetic fields are introduced to explain the flat rotational profile in the Sun (Brown et al. 1989; Kosovichev et al. 1997; Eggenberger et al. 2005; Yang & Bi 2006, 2008). However, gravity waves can also provide a satisfactory explanation for the solar rotation (Zahn et al. 1997; Talon & Charbonnel 2005). Especially for intermediate-mass stars which do not experience magnetic braking, our calculations show that rotational instabilities are efficient enough to transport angular momentum in these stars.

Table 1 The values of the parameters for angular momentum loss, the transport of angular momentum, and element mixing.

Parameter	f_k	β	$\Omega_{\rm crit}$	f_Ω	f_c
Value	$1.0^a(2.5^b)$	1.5	$5\Omega_\odot$	1.0	0.2

Notes: ^{a} for models with $M > 1.0\,M_\odot$; ^{b} for $1.0\,M_\odot$ model.

3 RESULTS

We used the Yale Rotation Evolution Code (YREC7) to compute the evolutions of rotating and non-rotating models with masses between 1.0 and 3.0 $M_\odot$. The code has been updated with latest input physics over the last three decades (Endal & Sofia 1976, 1978; Pinsonneault et al. 1989; Chaboyer et al. 1995; Yang & Bi 2007). The new OPAL EOS tables (Rogers & Nayfonov 2002), OPAL opacity tables (Iglesias & Rogers 1996), and the opacity tables for low temperature provided by Alexander & Ferguson (1994) were used. Energy transfer by convection is treated according to the standard mixing length theory. The value of 1.72 for the mixing-length parameter (α) was calibrated against the Sun. The initial chemical compositions in our models were fixed at $Z_0 = 0.02$ and $X_0 = 0.707$. The initial rotation period P_0 (or initial rotation velocity V_0) was a free parameter. We mainly computed the evolutions of the models with $P_0 = 0.74$ and 0.50 d. All models shared the same initial parameters except for mass and rotation period.

3.1 For Stars with Mass Less than 1.5 $M_\odot$

Figure 1 shows the evolutionary tracks of the $1.0\,M_\odot$ models with and without rotation. No matter what the initial rotation period is, the efficient magnetic braking results in almost the same rotational velocity (see panel a1 in Fig. 2) within a few hundred Myr, which leads to the fact that the evolutionary tracks of the two rotating models almost overlap in the Hertzsprung-Russell (HR) diagram. When the age of stars is younger than about 0.25 Gyr, the effective temperature and luminosity of the

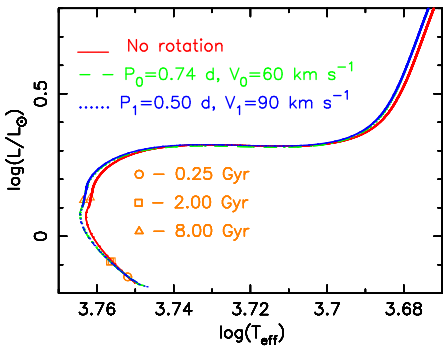

Fig. 1 Evolutionary tracks in the HR diagram for 1 $M_\odot$ models. The solid (*red*) line corresponds to the track of the non-rotating model, the dashed (*green*) and dotted (*blue*) lines show that of the rotating models with an initial period of 0.74 and 0.50 d, respectively. The positions of models at the ages of 0.25, 2.0, and 8.0 Gyr are marked on the tracks.

rotating models are slightly lower than those of the non-rotating ones. However, when age $>$ 0.25 Gyr, the effective temperature of the rotating models is higher but luminosity is lower than those of the non-rotating ones at the same age.

The rotational mixing takes effect only after composition gradients have been produced. When age $<$ 0.25 Gyr, the variation of chemical compositions with respect to radius is very small for a 1.0 $M_\odot$ model, thus the effects of rotational mixing can be neglected and the hydrostatic effects of rotation play a dominant role in this stage. The hydrostatic effects of rotation result in a decrease in the effective gravity of stars, which can slightly decrease the central temperature and enlarge the radius of rotating models compared to non-rotating ones. Therefore, the rotating models have a slightly lower luminosity and effective temperature than non-rotating ones.

When age > 0.25 Gyr (the central hydrogen abundance $X_c \lesssim 0.69$), due to angular momentum loss, on the one hand, the rotation rate becomes low enough to neglect the influences of the hydrostatic effects on the radius; on the other hand, the increase in the gradients of angular velocity and chemical compositions with respect to radius means that the rotational mixing begins to play a dominant role by feeding more fresh hydrogen fuel into the hydrogen-burning region and by transporting helium outwards, which can lead to an increase in the mean density, i.e. decrease in radius, and deceleration of evolution. Thus the rotating models exhibit a higher central hydrogen abundance (see panel a in Fig. 3) and effective temperature but slightly lower luminosity than non-rotating ones at the same age. When the models evolved to the same evolutionary state (the same central hydrogen abundance), the luminosity of rotating models is only slightly higher than that of non-rotating ones by consuming more hydrogen, however the radius of rotating models is still smaller than that of non-rotating ones (see panel a2 in Fig. 2) due to the effects of the rotational mixing, therefore the effective temperature of rotating models is higher than that of non-rotating ones (see panels a1 and a2 in Fig. 4). If the rotational mixing is not considered, Figure 5 shows that rotation has almost no effect on the evolution of a 1.0 $M_\odot$ model after the age of 0.25 Gyr.

In Figure 6, we show the evolutionary tracks of rotating and non-rotating models with $M =$ 1.2 and 1.4 $M_\odot$. The effects of rotation on the evolution of these stars are similar to those on the evolution of the 1.0 $M_\odot$ model. Compared with the tracks of non-rotating models, the tracks of rotating models move to the left of the HR diagram. For stars with $M \lesssim 1.4\,M_\odot$, due to the efficient magnetic braking, the hydrostatic effects of rotation play a dominant role after only about 100 Myr. Then, just as in the case of 1.0 $M_\odot$ models, the rotational mixing begins to play a dominant role. The rotating models exhibit a higher effective temperature and an approximately equal luminosity

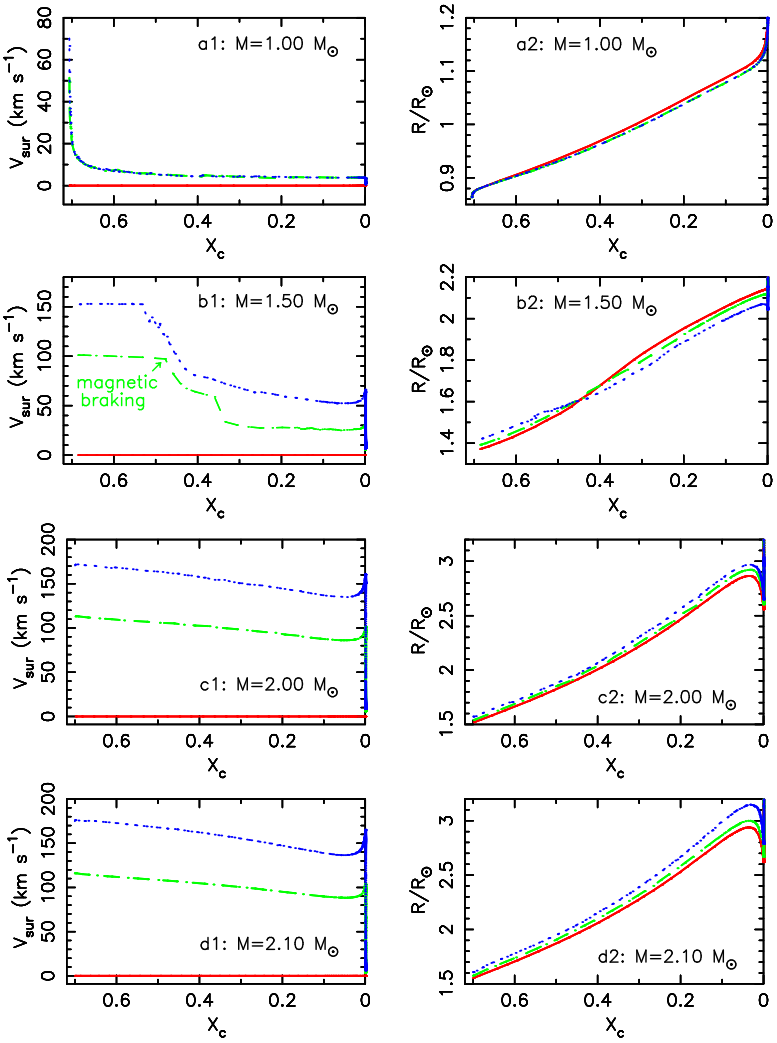

Fig. 2 The surface (equatorial) velocity and radius as a function of the mass fraction of central hydrogen. The solid (*red*) line corresponds to the non-rotating model, and the dashed (*green*) and dotted (*blue*) lines indicate the rotating models with an initial period of 0.74 and 0.50 d, respectively.

compared to the non-rotating ones when they have evolved into the same evolutionary state [for instance the beginning of the MS hook (Yang et al. 2011a) in the HR diagram]. Moreover, for the star with M =1.4 $M_{\odot}$, Figure 6 demonstrates that the rotating models have higher effective temperatures and luminosities at the age of 1.0 Gyr but have lower effective temperatures at the age of 1.75 Gyr than non-rotating ones, and that the rotating models evolve faster than the non-rotating ones. This is different from the evolutions of the models with M =1.0 $M_{\odot}$.

The radiative temperature gradient can be changed by the Von Zeipel (1924) effect, and the adiabatic temperature gradient can be influenced by the mixing of elements caused by hydrostatic instabilities. Thus the instability of convection can be influenced by the effects of rotation. Our calculations show that the effects of rotation can result in a decrease in the radius or mass of the convective core for stars with 1.1 $M_{\odot} \lesssim M < 2.05\, M_{\odot}$ but an increase for stars with $M > 2.05\, M_{\odot}$

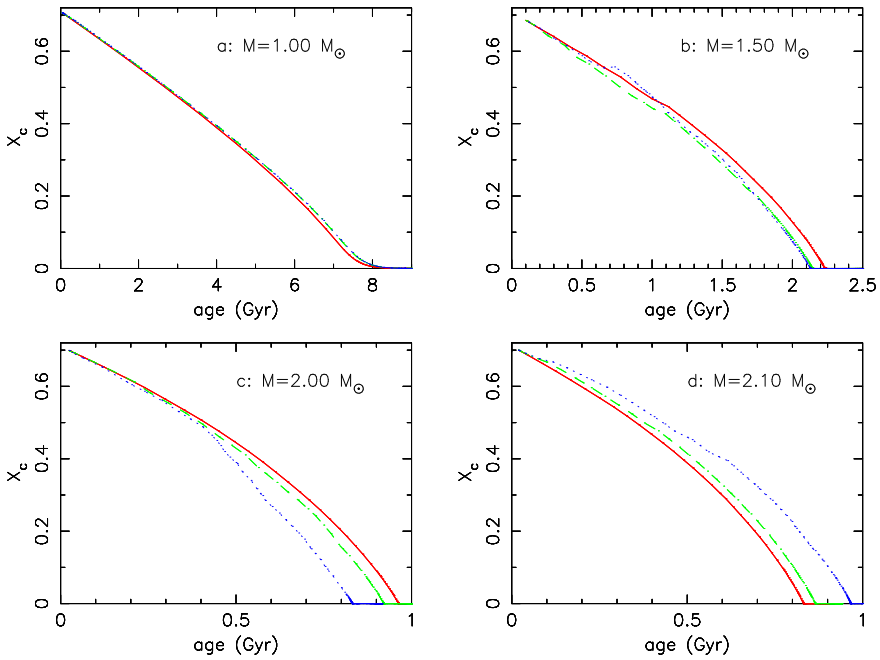

Fig. 3 The mass fraction of central hydrogen as a function of age. The solid (*red*) line corresponds to the non-rotating model, the dashed (*green*) and dotted (*blue*) lines show the rotating models with an initial period of 0.74 and 0.50 d, respectively.

(see Fig. 7). The decrease in the convective core leads to the fact that the hydrogen abundance in the convective core of rotating models decreases faster than that of non-rotating ones. Although the rotational mixing can bring hydrogen fuel into the core from outer layers, it cannot compensate for the decrease of the central hydrogen caused by the decrease in the convective core. As a consequence, the rotating models evolve faster than non-rotating ones during the MS stage for stars with 1.1 $M_\odot \lesssim M \lesssim 2.0\, M_\odot$ (see Fig. 3). Furthermore, Figure 7 shows that the faster the rotation, the smaller the convective core, thus the faster the evolution of the MS stage for stars with 1.1 $M_\odot \lesssim M \lesssim 2.0\, M_\odot$. We named this phenomenon "rotation acceleration." The rotation acceleration leads to the fact that the rotating models with $M = 1.4\, M_\odot$ exhibit higher luminosities at the age of 1.0 Gyr and lower effective temperatures at the age of 1.75 Gyr than the non-rotating ones (see Fig. 6).

3.2 For Stars with Masses between 1.5 and 1.7 $M_\odot$

Figure 8 shows the evolutionary tracks of the rotating and non-rotating models with $M = 1.5$, 1.6, and 1.7 $M_\odot$. For stars with $M \gtrsim 1.5\, M_\odot$, their envelopes are radiative at the beginning of MS. Before the appearance of the convective envelope (i.e. before magnetic braking), the stars maintain a fast rotation (see panel b1 in Fig. 2), the hydrostatic effects of rotation dominate the corrections to the models and result in the rotating models having a larger radius (see panel b2 in Fig. 2) and slightly lower central temperature than the non-rotating ones, thus the rotating models have a slightly lower luminosity and effective temperature than the non-rotating ones at the same evolutionary stage in the early stage of the MS (see panels b1 and b2 in Fig. 4). However due to the effects of acceleration in rotation, as the evolution proceeds, the rotating models can exhibit a slightly higher luminosity than non-rotating ones at the same age.

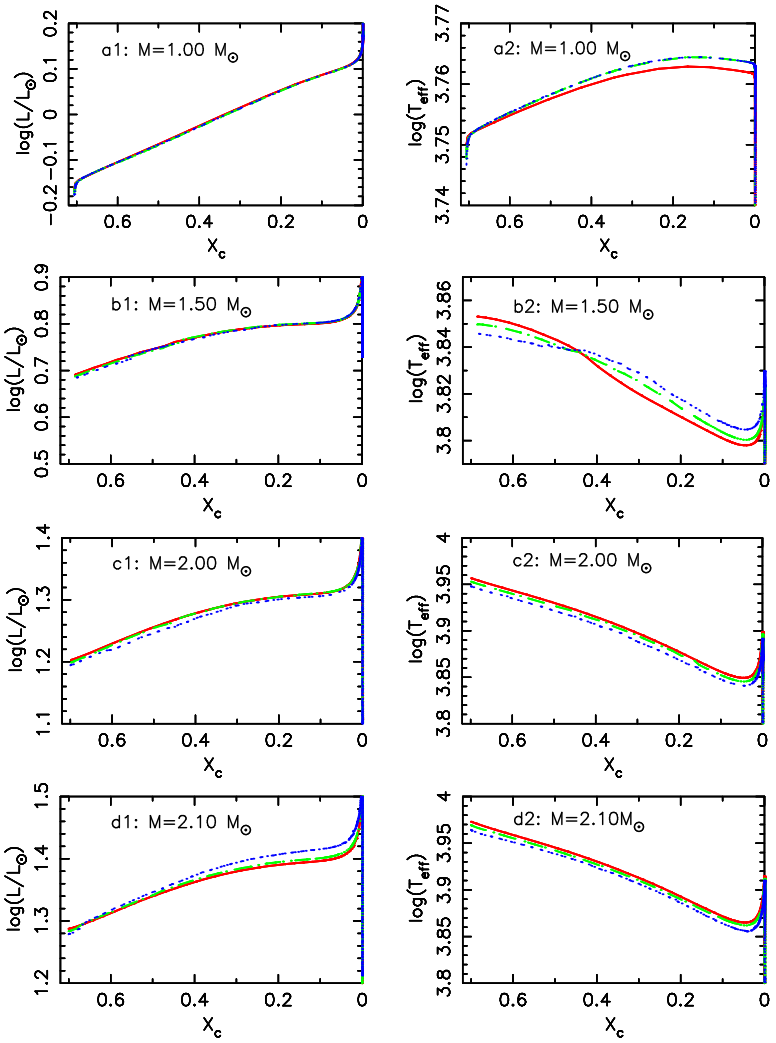

Fig. 4 The luminosity and effective temperature as a function of the mass fraction of central hydrogen. The solid (*red*) line corresponds to the non-rotating model, and the dashed (*green*) and dotted (*blue*) lines indicate the rotating models with an initial period of 0.74 and 0.50 d, respectively.

After the convective envelope has developed, due to the angular momentum loss, on the one hand, the rotation of the stars begins to slow, which results in a reduction in the hydrostatic effects of rotation (for example stellar radius is almost no longer affected by the hydrostatic effects of rotation); on the other hand, the gradient of angular velocity with respect to radius increases, which enhances the effects of rotational mixing. As the evolution proceeds, the rotational mixing begins to play a dominant role, thus the radius of rotating models changes from larger to smaller than that of non-rotating ones (see panel b2 in Fig. 2). In addition, when the models with and without rotation are evolved to the same evolutionary state of the MS stage, their luminosities are approximately equal, therefore the effective temperatures of rotating models change from lower to higher compared to that of non-rotating ones (see panel b2 in Fig. 4). However, before the MS hook of stars with

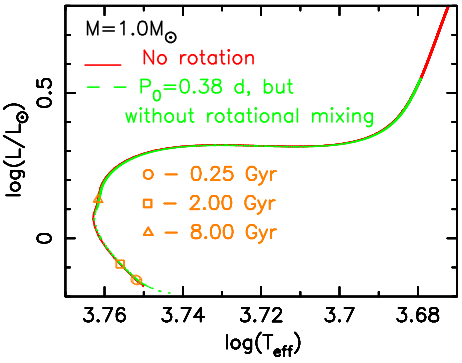

Fig. 5 Same as Fig.1 but using the rotating model without including the effects of rotational mixing.

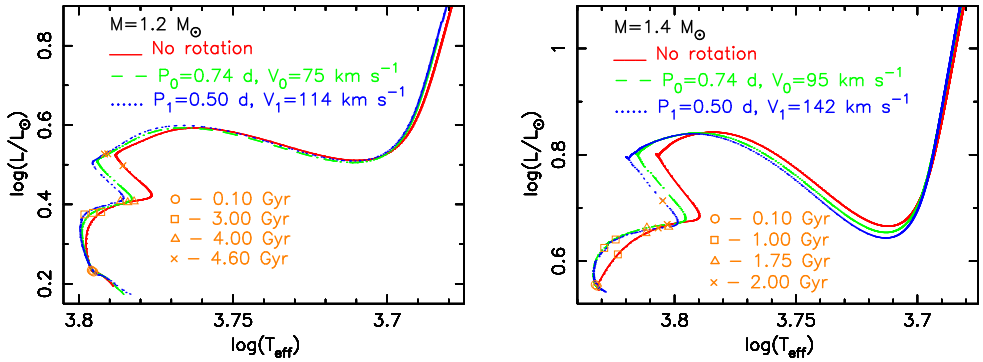

Fig. 6 Same as Fig.1 but for stars with $M = 1.2$ and $1.4\,M_{\odot}$, respectively.

$M \gtrsim 1.6\,M_{\odot}$, due to the facts that magnetic braking occurs in the late stage of the MS and rotation accelerates the evolutions of rotating models, the effective temperature of rotating models is always lower than that of non-rotating ones at the same age. For example, at the age of 1.5 Gyr, the effective temperature of the star with $M = 1.6\,M_{\odot}$ is about 6620 K for the non-rotating model but is 6540 K for the rotating model with $T_0 = 0.74$ d. The difference in the effective temperatures is 80 K.

Moreover, Figure 8 shows that the luminosities of rotating models are slightly higher than those of the non-rotating ones at the end of the MS hook. This is because rotation hardly affects the convective core when $X_c < 0.1$ for these stars and the rotational mixing makes rotating models consume slightly more hydrogen than non-rotating ones during the MS hook.

3.3 For Stars with Masses between 1.8 and 2.0 $M_{\odot}$

The evolutionary tracks of the rotating and non-rotating models with $M = 1.8$ and $2.0\,M_{\odot}$ are shown in Figure 9. For these stars, the rotating models exhibit slightly lower luminosities and effective temperatures than non-rotating ones when they reached the same evolutionary state during the entire MS stage (see panels c1 and c2 in Fig. 4). Before the MS hook, even at the same age the effective temperatures of the rotating models are also lower than those of the non-rotating ones, but their luminosities are approximately equal. For example, for the star with $M = 1.8\,M_{\odot}$, at the age of 1.1 Gyr the effective temperature and luminosity are 6970 K and $13.03\,L_{\odot}$ for the non-rotating

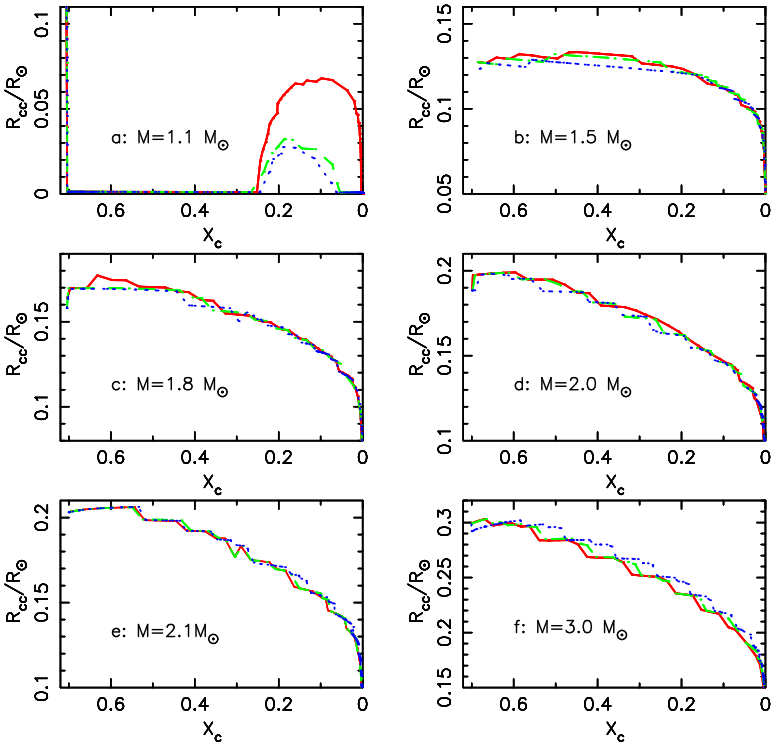

Fig. 7 The radius of the convective core as a function of the mass fraction of central hydrogen abundance. The solid (*red*) line corresponds to the non-rotating model, and the dashed (*green*) and dotted (*blue*) lines indicate the rotating models with an initial period of 0.74 and 0.50 d, respectively.

model but 6670 K and 13.08 $L_\odot$ for the rotating model with $T_0 = 0.5$ d, respectively. The difference in the effective temperatures is about 300 K. This is because these stars do not experience magnetic braking during the MS stage. The fast rotation leads to the fact that the hydrostatic effects of rotation dominate the corrections to radius. In addition, the effects of the mixing caused by rotationally induced instabilities are partly counteracted by the effect of the decrease in the convective core in these models. Thus the rotating models have a larger radius than non-rotating ones at the same evolutionary state (see panel c2 in Fig. 2). Moreover, the hydrostatic effects of fast rotation also lead to a decrease in the central temperature. For example, when the star with $M = 2.0\,M_\odot$ evolved to $X_c = 0.2607$, the central temperature is 2.2978×10^7 K for the non-rotating model but is 2.2966×10^7 K for the rotating model with $P_0 = 0.5$ d. The lower the central temperature, the lower the energy produced by H-burning. Thus the rotating models have slightly lower luminosities than non-rotating ones at the same evolutionary state. As a consequence, the effective temperatures of rotating models are lower than those of non-rotating ones.

3.4 For the Stars with Mass Larger than 2.1 $M_\odot$

In Figure 10, we show the evolutionary tracks of the 2.1 and 3.0 $M_\odot$ models with and without rotation. For stars with $M \geq 2.1\,M_\odot$, in the early stage of the MS ($X_c > 0.5$ for $M = 2.1\,M_\odot$ and $X_c > 0.6$ for $M = 3.0\,M_\odot$) the hydrostatic effects of rotation dominate the corrections to stellar models; thus the rotating models exhibit lower luminosities and effective temperatures than the non-rotating ones at the same age.

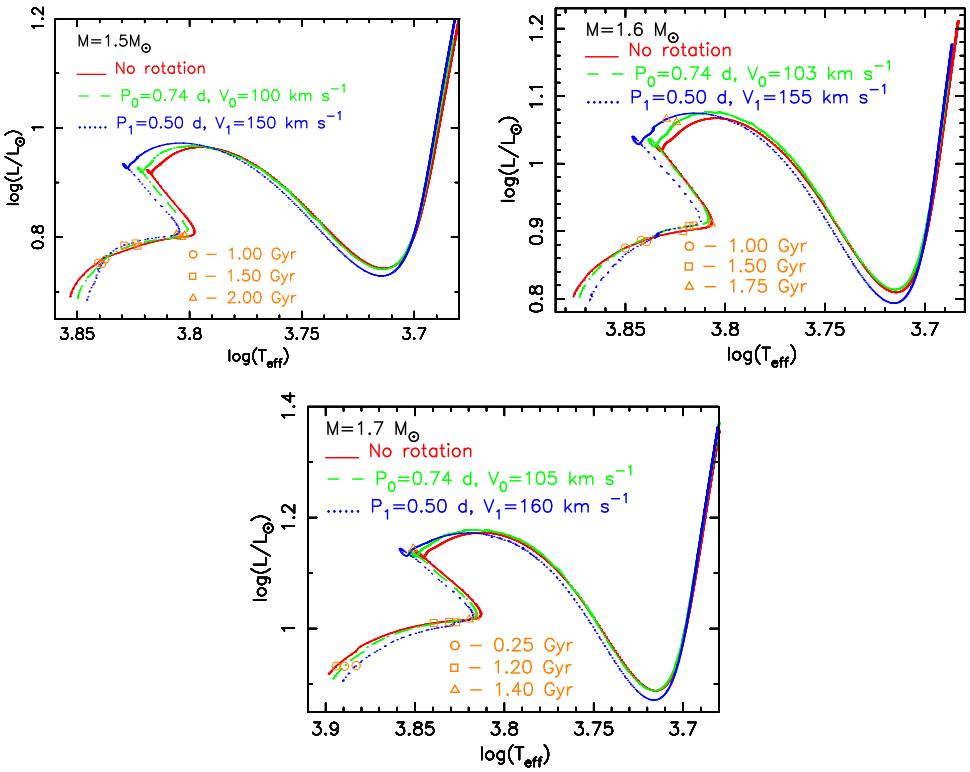

Fig. 8 Same as Figure 1 but for stars with $M = 1.5$, 1.6, and 1.7 $M_{\odot}$, respectively.

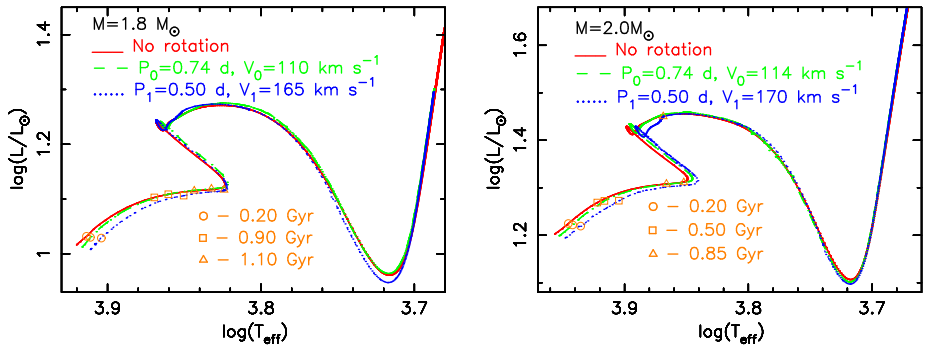

Fig. 9 Same as Figure 1 but for the models with $M = 1.8$ and 2.0 $M_{\odot}$, respectively.

As the evolution proceeds, the effects of rotation lead to an increase in the convective core for these stars, and the more massive the star or the higher the rotation rate, the larger the change in the convective core (see Fig. 7). Both the increase in the convective core and rotational mixing can enhance the hydrogen abundance and decrease the helium abundance in the core, which leads to an increase in the mean density (i.e. a decrease in radius) and decrease in the central temperature of the rotating models compared to non-rotating ones at the same age, and prolongs the lifetime of core

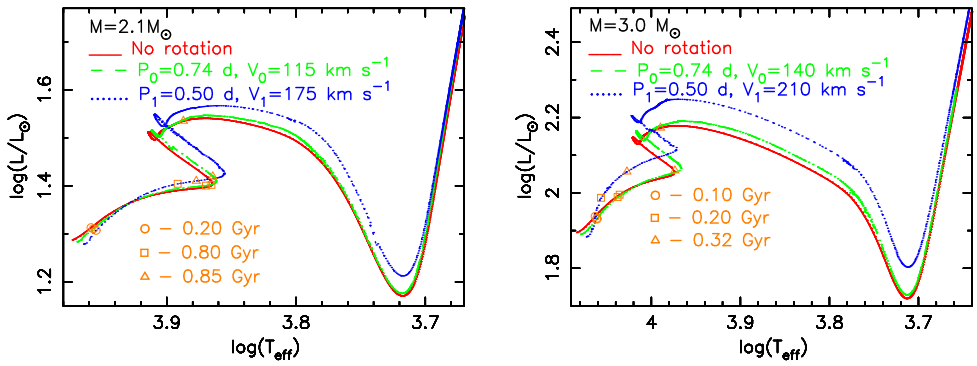

Fig. 10 Same as Fig. 1 but for the models with $M = 2.1$ and $3.0\,M_{\odot}$, respectively.

H burning. In addition, the hydrostatic effects of rotation can also lead to a decrease in the central temperature. Thus rotating models evolve more slowly than non-rotating ones and exhibit lower luminosities than non-rotating ones at the same age. The effects of rotation result in an increase in the convective core for stars with $M \gtrsim 2.1\,M_{\odot}$ but a decrease in the convective core for stars with $M \lesssim 2.0\,M_{\odot}$. Chemical elements are completely mixed in the convective cores. The increase of the convective core causes the location of the chemical element gradient to move outwards, which leads to the process where the product of H-burning can be transported outwards much more efficiently by rotational mixing. Thus the rotationally induced element mixing in stars with $M \gtrsim 2.1\,M_{\odot}$ is more efficient than that in stars with mass between about 1.7 and $2.0\,M_{\odot}$. For example, when the stars with $M = 2.0$ and $2.1\,M_{\odot}$ evolved to $X_c = 0.261$, the surface hydrogen abundance is 0.707 for both non-rotating models, however it is 0.705 for the rotating model with $M = 2.0\,M_{\odot}$ and $P_0 = 0.5$ d and is 0.700 for the rotating model with $M = 2.1\,M_{\odot}$ and $P_0 = 0.5$ d. The efficient mixing leads to the fact that the radius of the rotating models is smaller than that of non-rotating ones at the same age and the change of the radius is larger than that of luminosity. Thus the rotating models exhibit higher effective temperatures than non-rotating ones at the same age during the middle stage of MS. However, when the models evolved into the same evolutionary state in the late stage of MS, because the rotating models consumed more hydrogen fuel than non-rotating ones, which can enhance the temperatures of the core and the He-core mass left behind, the rotating models produce more energy from H burning than non-rotating ones. The more energy is produced, the more the stars expand. Thus the rotating models exhibit larger radii and lower effective temperatures than non-rotating ones at the same evolutionary state. The effects of rotation on the evolution of these stars with $M \gtrsim 2.1\,M_{\odot}$ are similar to the effects of convective core overshooting.

4 DISCUSSION AND CONCLUSIONS

Besides the influences of rotation on the internal evolution of stars, effects of rotation on the observable parameters of stars depend on the product $v \sin i$, where v is the equatorial rotational velocity and i refers to the angle between the rotational axis of a star and the direction towards the observer. In this work, we only focus on the effects due to internal stellar evolution.

The effects of rotation on stellar structure and evolution are mainly derived from hydrostatic effects, the mixing of elements caused by rotationally induced instabilities, and the Von Zeipel effect which influences the instability of convection by changing the radiative temperature gradient. The hydrostatic effects mainly lead to an increase in radius and a decrease in the effective temperature. The mixing of elements, however, chiefly results in an increase in the mean density, i.e. a decrease in radius and an increase in the effective temperature. Moreover, rotation leads to a decrease in the

convective core for stars with $M < 2.05\,M_{\odot}$, which can counteract the effects of the rotational mixing and accelerate the evolution of stars. However, rotation results in an increase in the convective core for stars with $M > 2.05\,M_{\odot}$, which dominates that of rotation on the evolutions of these stars. For the models with masses between about 1.7 and 2.0 $M_{\odot}$, because the effect of the rotational mixing is counteracted by the effects of the decrease in the convective core and they do not experience magnetic braking during the MS stage, the hydrostatic effects dominate the effects on the effective temperatures and luminosities of these models; thus, the effective temperatures and luminosities of rotating models are lower than those of non-rotating ones during the MS stage.

The evolutions of our rotating models with $M \gtrsim 2.1\,M_{\odot}$ are consistent with the calculation results of Eggenberger et al. (2010) and Girardi et al. (2011). However the rotating models with mass between $\sim$1.7 and 2.0 $M_{\odot}$ manifest lower effective temperatures than non-rotating ones, which is not consistent with the results of Girardi et al. (2011) but is similar to the calculation result of Bastian & de Mink (2009). Moreover, in our models, the MS bandwidth of rotating models with $M > 2.0\,M_{\odot}$ is wider than that of non-rotating ones. However, the MS bandwidth of rotating models with $M < 2.0\,M_{\odot}$ is narrower than that of non-rotating ones, which is consistent with the distributions of the large sample of rotating stars collected by Royer et al. (2007) in the HR diagram (see fig. 4 of Zorec & Royer 2012). In the next work, we will give a more detailed comparison.

For MS stars with a given rotation rate, the change in the effective temperature caused by rotation increases with increasing mass. For example, when age$= 1.1$ Gyr and $P_0 = 0.5$ d, the difference in the effective temperature between the non-rotating and rotating model is about 300 K for stars with mass between 1.7 and 1.8 $M_{\odot}$, around 200 K for stars with $M = 1.6\,M_{\odot}$, and about 40 K for stars with $M = 1.5\,M_{\odot}$, but the difference is only several Kelvin for stars with $M \lesssim 1.4\,M_{\odot}$. The change in the effective temperature caused by rotation decreases with decreasing mass. Thus, for some intermediate-age star clusters, rotation might lead to a color spread near the MSTO in their CMD. In the next work, we will discuss the isochrone of rotating models.

In this work, we calculated a grid of evolutionary tracks of rotating models with masses between 1.0 and 3.0 $M_{\odot}$ and resolution $\delta M \leq 0.02\,M_{\odot}$. We find that the effects of rotation on stellar structure and evolution are dependent not only on the rotation rate but also on the mass of stars. For stars with $M > 2.05\,M_{\odot}$, rotation leads to an increase in the convective core and prolongs the lifetime of core H burning; the evolution of rotating models for these stars is slower than that of non-rotating ones; in the early stage of MS, the changes in luminosities and effective temperatures are mainly due to the hydrostatic effects of rotation, thus rotating models exhibit lower luminosities and effective temperatures than non-rotating ones at the same age; however, in the late stage of MS, rotating models can manifest higher effective temperatures than non-rotating ones at the same age and larger luminosities at the same evolutionary stage because the rotational mixing dominates the effects on the models. For stars with $1.1\,M_{\odot} \lesssim M < 2.05\,M_{\odot}$, rotation results in a decrease in the convective core and shortens the lifetime of core H burning; the rotating models of these stars evolve faster than non-rotating ones. When $1.7\,M_{\odot} \lesssim M < 2.05\,M_{\odot}$, the rotating models exhibit lower effective temperatures but approximately equal luminosities compared to non-rotating ones at the same age; the evolutionary tracks of the rotating models are located to the lower right of non-rotating ones in the HR diagram, and are mainly due to the hydrostatic effects of rotation and "rotation acceleration." However, for stars with $1.0\,M_{\odot} \lesssim M \lesssim 1.4\,M_{\odot}$, due to the fact that these stars experienced magnetic braking from the beginning of evolution, the rotational mixing and "rotation acceleration" dominate the effects of rotation on the evolution of these stars; the evolutionary tracks of rotating models for these stars are mainly located to the left of non-rotating ones in the HR diagram; the rotating models can exhibit lower or higher effective temperatures than non-rotating ones at the same age, which depends on the mass and age of stars. Our calculations show that the mass of $2.05\,M_{\odot}$ is a critical value for the effect of rotation on the stellar structure and evolution. This value is very close to the critical mass ($2.01\,M_{\odot}$) for oscillations in horizontal branch stars (Yang et al. 2012). Rotation could lead to a color spread for some intermediate-age star clusters near the MSTO in their CMD.

Acknowledgements This work was supported by the China Postdoctoral Science Foundation (Grant No. 20100480222), the National Natural Science Foundation of China (Grant Nos. 11273012, 11273007, 10933002 and 11003003), and the Project of Science and Technology from the Ministry of Education (211102).

References

Alexander, D. R., & Ferguson, J. W. 1994, ApJ, 437, 879
Bastian, N., & de Mink, S. E. 2009, MNRAS, 398, L11
Bekki, K., & Mackey, A. D. 2009, MNRAS, 394, 124
Brown, T. M., Christensen-Dalsgaard, J., Dziembowski, W. A., et al. 1989, ApJ, 343, 526
Chaboyer, B., Demarque, P., & Pinsonneault, M. H. 1995, ApJ, 441, 865
Eggenberger, P., Maeder, A., & Meynet, G. 2005, A&A, 440, L9
Eggenberger, P., Miglio, A., Montalban, J., et al. 2010, A&A, 509, A72
Endal, A. S., & Sofia, S. 1976, ApJ, 210, 184
Endal, A. S., & Sofia, S. 1978, ApJ, 220, 279
Fricke, K. 1968, ZAp, 68, 317
Girardi, L., Eggenberger, P., & Miglio, A. 2011, MNRAS, 412, L103
Goldreich, P., & Schubert, G. 1967, ApJ, 150, 571
Goudfrooij, P., Puzia, T. H., Kozhurina-Platais, V., & Chandar, R. 2009, AJ, 137, 4988
Goudfrooij, P., Puzia, T. H., Kozhurina-Platais, V., & Chandar, R. 2011, ApJ, 737, 3
Iglesias, C. A., & Rogers, F. J. 1996, ApJ, 464, 943
Kawaler, S. D. 1988, ApJ, 333, 236
Kippenhahn, R., & Thomas, H.-C. 1970, in IAU Colloq. 4: Stellar Rotation, ed. A. Slettebak, 20 (New York: Gordon and Breach), 1970
Kosovichev, A. G., Schou, J., Scherrer, P. H., et al. 1997, Sol. Phys., 170, 43
Mackey, A. D., & Broby Nielsen, P. 2007, MNRAS, 379, 151
Mackey, A. D., Broby Nielsen, P., Ferguson, A. M. N., & Richardson, J. C. 2008, ApJ, 681, L17
Maeder, A., & Meynet, G. 2000, ARA&A, 38, 143
Meynet, G., & Maeder, A. 1997, A&A, 321, 465
Milone, A. P., Bedin, L. R., Piotto, G., & Anderson, J. 2009, A&A, 497, 755
Pinsonneault, M. H., Kawaler, S. D., Sofia, S., & Demarque, P. 1989, ApJ, 338, 424
Platais, I., Melo, C., Quinn, S. N., et al. 2012, ApJ, 751, L8
Rogers, F. J., & Nayfonov, A. 2002, ApJ, 576, 1064
Royer, F., Zorec, J., & Gómez, A. E. 2007, A&A, 463, 671
Rubele, S., Girardi, L., Kozhurina-Platais, V., Goudfrooij, P., & Kerber, L. 2011, MNRAS, 414, 2204
Rubele, S., Kerber, L., & Girardi, L. 2010, MNRAS, 403, 1156
Talon, S., & Charbonnel, C. 2005, A&A, 440, 981
Thoul, A. A., Bahcall, J. N., & Loeb, A. 1994, ApJ, 421, 828
von Zeipel, H. 1924, MNRAS, 84, 665
Yang, W. M., & Bi, S. L. 2006, A&A, 449, 1161
Yang, W. M., & Bi, S. L. 2007, ApJ, 658, L67
Yang, W.-M., & Bi, S.-L. 2008, ChJAA (Chin. J. Astron. Astrophys.), 8, 677
Yang, W., Li, Z., Meng, X., & Bi, S. 2011a, MNRAS, 414, 1769
Yang, W., Meng, X., Bi, S., et al. 2011b, ApJ, 731, L37
Yang, W., Meng, X., Bi, S., et al. 2012, MNRAS, 422, 1552
Yoon, S.-C., Langer, N., & Norman, C. 2006, A&A, 460, 199
Zahn, J.-P. 1992, A&A, 265, 115
Zahn, J.-P., Talon, S., & Matias, J. 1997, A&A, 322, 320
Zorec, J., & Royer, F. 2012, A&A, 537, A120